ARCHIVES OF ELECTRICAL ENGINEERING VOL. 63(2), pp. 211-225 (2014)

DOI 10.2478/aee-2014-0017

Analysis of the proximity and skin effects on copper loss in a stator core

ADRIAN MŁOT [1], MARIUSZ KORKOSZ[2], PIOTR GRODZKI[2], MARIAN ŁUKANISZYN[1]

[1]*Faculty of Electrical Engineering, Automatic Control and Informatics, Opole University of Technology*
Prószkowska 76, 45-758 Opole, Poland
[2]*Rzeszow University of Technology, The Faculty of Electrical and Computer Engineering*
W. Pola 2, 35-959 Rzeszów, Poland
e-mail: m.lukaniszyn@po.opole.pl

(Received: 26.11.2013, revised: 12.02.2014)

Abstract: Accurate prediction of power loss distribution within an electrical device is highly desirable as it allows thermal behavior to be evaluated at the early design stage. Three-dimensional (3-D) and two-dimensional (2-D) finite element analysis (FEA) is applied to calculate dc and ac copper losses in the armature winding at high-frequency sinusoidal currents. The main goal of this paper is showing the end-winding effect on copper losses. Copper losses at high frequency are dominated by the skin and proximity effects. A time-varying current has a tendency to concentrate near the surfaces of conductors, and if the frequency is very high, the current is restricted to a very thin layer near the conductor surface. This phenomenon of nonuniform distribution of time-varying currents in conductors is known as the skin effect. The term proximity effect refers to the influence of alternating current in one conductor on the current distribution in another, nearby conductor. To evaluate the ac copper loss within the analyzed machine a simplified approach is adopted using one segment of stator core. To demonstrate an enhanced copper loss due to ac operation, the dc and ac resistances are calculated. The resistances ratio ac to dc is strongly dependent on frequency, temperature, shape of slot and size of slot opening.

Key words: end-winding, copper loss, iron loss, ac loss, skin effect, proximity effect

1. Introduction

There are two principal mechanisms for losses in high speed ac motors at high frequency, that are iron losses and copper losses. The most significant losses come from the winding due to copper resistance. High speed motors at high-frequency sinusoidal current waveform, which can make the effective winding resistance very high and for that reason copper losses are increasing when frequency grows [1, 2]. The winding resistance of high speed motor is a result of both skin and proximity effects [2-5]. The main phenomenon that leads to ac losses is the skin effect which is the tendency for high-frequency currents to flow on the surface of a conductor. The skin effect can be mitigated through the use of smaller conductor strands.

Alternating currents at high frequency are confined to a thin layer at the surface of the conductor due to the skin effect. The general theory shows that the current penetrates a depth δ that can be expressed:

$$\delta = \sqrt{\frac{2}{\omega\mu\sigma}} = \frac{1}{\sqrt{\pi f \mu_o \mu_r \sigma}}, \tag{1}$$

where ω is the frequency of the applied field, μ is the permeability, and σ is the conductivity of the conductor. The second phenomenon is the proximity effect which is the tendency for current to flow in other undesirable patterns that form localised current loops or concentrated distributions due to the presence of a magnetic field generated by nearby conductors. The proximity effect can be mitigated by transposing conductor strands. Both of these are the well-known current-displacement effects within electrical machines, transformers and inductors.

During high rotating flux at high frequencies, the ac resistance can be prominent, usually exceeding dc resistance and resulting in high copper losses. With slot opening machines, the magnetic field near the gap produces a strong local proximity effect and can produce very high ac copper resistance and losses. Also, the strands placed in the rear slot in the corners can produce higher losses than others strands, due to flux leakage crossing slot from back iron to tooth. Power loss in any electric machines with magnetic fields, is the sum of this effects (dc loss and ac loss), and the design process is made more difficult by their relationship to one another. For instance, one of the common methods for reducing ac resistance is the Litz wire, and that method greatly reduces the cross-sectional area of the conductor and drastically increases dc resistance [6, 7]. Additionally the big open slot can cause significant losses in conductors, even at a small amount of ac current. Using a powdered core with no gap will substantially reduce proximity effects and the resulting ac copper losses. Also, different arrangement conductors in slots, different shapes of cross-section conductors and/or changes in a gap-width can change the current distribution in the winding and minimize the skin and proximity effects.

2. Copper and iron losses analysis in a stator core

The total winding loss P_{cu} is broken up into two components. These are the dc loss (P_{dc}), and the ac loss (P_{ac}). The maximum current a winding can carry is limited by the total losses generated by the current itself. As a minimum, the total losses are called P_{dc} which represent the ohmic losses of a conductor current (RMS value of dc or ac currents), and from the Ohm law the dc resistance can be expressed as:

$$R_{dc} = P_{dc} / I^2 . \tag{2}$$

P_{dc} is defined as the winding loss at 10 Hz, including dc or low frequency current flowing through the conductors. Hence there is RMS losses only. If the winding carries an alternating current this current causes eddy-current inside the conductors, and P_{ac} is defined due to high

frequency skin and proximity effect. Also this P_{ac} loss strongly depends on conductor geometry. However, if eddy currents occur, they cause additional losses called eddy-current losses. From the total copper losses as the sum of P_{dc} and eddy current losses, the R_{ac} resistance can be written as:

$$R_{ac} = P_{ac} / I^2 . \tag{3}$$

From (2-3) an equivalent bulk value of the ac winding losses under sinusoidal RMS current is found by (4). This bulk value of the ac copper loss is used to determine the increase of resistance or copper loss under ac excitation as compared to dc operation. The ratio of the equivalent ac resistance or copper loss to the ideal dc value R_{ac}/R_{dc} (P_{ac}/P_{dc}) is a commonly used figure of merit to assess high frequency effects [8].

$$P_{ac} = \frac{R_{ac}}{R_{dc}} \frac{\rho \cdot l}{S} i_{rms}^2, \tag{4}$$

where i_{rms} is the RMS current, ρ is the resistivity of medium, l is the length of copper wire and S is the cross section of conductor.

The copper power losses (P_{dc}, P_{ac}) in the solid conductors are determined in FEA from the Joule loss law:

$$P_{Copper} = \iiint_V \mathbf{E} \cdot \mathbf{J} \, dV = \rho \iiint_V \mathbf{J}^2 dV = l\rho \iint_S J^2 dS. \tag{5}$$

The iron losses are calculated in a magnetic region of motor armature during 3-D FEA. The losses are a sum of three aspects such as the hysteresis losses, the Joule losses and excess losses. In the harmonic state, the iron losses are expressed by:

$$P_{Fe} = \iiint_V \left(k_h B_m{}^2 f + \frac{\sigma \pi^2 d}{6} (B_m f)^2 + k_e (B_m f)^{3/2} \cdot 8{,}67 \right) k_f \, dV, \tag{6}$$

where B_m is the maximum flux density, f the frequency, ρ resistivity of medium, σ iron conductivity, d the lamination sheet thickness, k_f packing factor, k_h the coefficient of hysteresis and k_e the coefficient of excess loss. To determine the coefficients of hysteresis and excess loss, it is needed to refer to the data supplied by sheet manufacturers. The data provide the iron losses in watts per kilogram for given flux density and a given frequency. Base on this data the loss coefficient k_h and k_e can be identified and used to compute iron losses and are reported in Table 1 for iron sheet M470 50 A at 50 Hz.

3. Test rig

For this experiment, several winding arrangements are investigated and one of them was built and tested. The prototype is based on armature core, that was constructed using the ferrite core of material M470 50 A with a 13 mm air-gap slot opening.

Table 1. Material coefficients for M470-50 A lamination

Description		Value	
Hysteresis coefficient	k_h	143	$Ws/T^2/m^3$
Electric conductivity	σ	2.5641e6	$(\Omega m)^{-1}$
Lamination thickness	d	0.5e-3	m
Excess loss coefficient	k_e	2.6	$W/(Ts^{-1})^{3/2}/m^3$
Packing factor	k_f	0.96	–
Mass density at 20°C	ρ	7760	kg/m^3

The cross section of the coil version I, and stator core is shown in Figure 1. Standard conductors were constructed of 7 turns wound on one stator tooth in series and consisted of six-strand parallel conductors. This particular example of winding version I (only one coil considered) is producing a copper loss of 26 W (10 Hz) to 46 W (800 Hz) at 80 Arms, and at winding temperature assumed to 25°C.

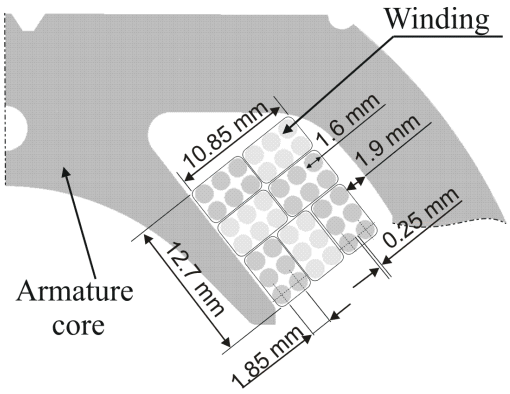

Fig. 1. The armature cross section of investigated motor with winding and dimensions

To evaluate the ac copper loss in the analysed machine a simplified approach is adopted utilizing the stator cores (Fig. 2a-b). Several stator cores were connected together (Fig. 2c) to increase active-length of strands wound onto the tooth, and demonstrate high impact of proximity and skin effects on copper loss. To simplify the winding of turns onto the tooth, the stator core was cut in half as shown in Figure 2c. To understand the behaviour of circulating eddy-currents in the solid conductors along the active-length and in the end-winding regions, the mutual coupling between phases which affect the proximity loss is not taken into account. Also, the influence of the rotor was assumed to be negligible.

Figure 3a presents the investigated coil (winding version IV, see Fig. 5) wound onto the tooth. The analysed version of coil is representative of mush winding comprising of 6 parallel conductor strands with 7 turns in series, where the location of the conductors are precisely defined by banding them in a defined position in the slot. The distribution of the conductors is accurately represented due to the provided method for winding of the conductors 'hand in hand' with a string to keep the strands together (Fig. 3b). This allows the arrangements of conductors in the slots for tested winding to be accurately reproduced in the FE model.

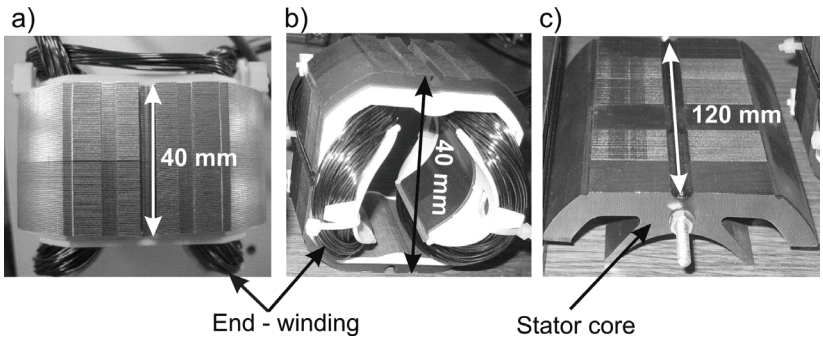

Fig. 2. Stator core used to analyse power loss (a-b) and the three cores were connected together in preparation winding the coils (c)

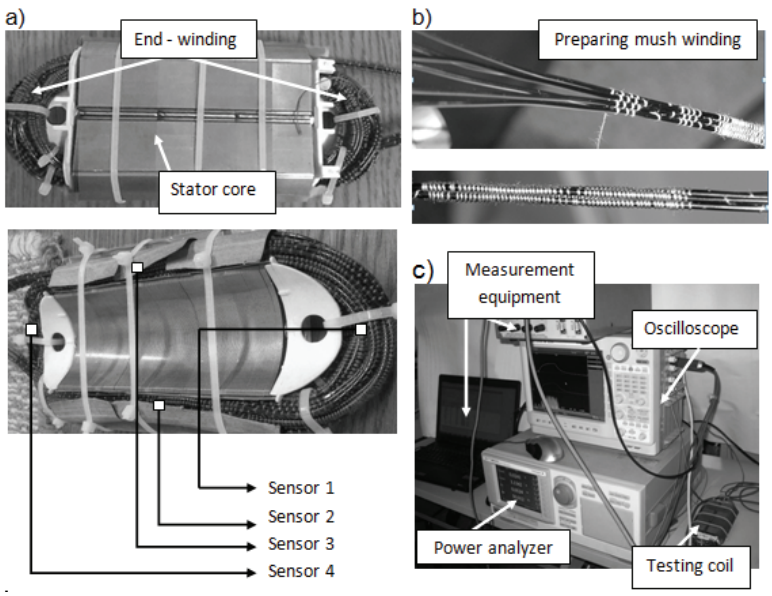

Fig. 3. Analysed segment of stator core with wounded coil of winding version IV (a), preparing mush (b) and test rig for copper and iron loss calculation (c)

Figure 3c presents the one-tooth segment test rig including an ac and/or dc power supply, oscilloscope, measurement equipment, thermocouples, power analyzer, and the tooth assembly. A thermal insulation chamber emulating adiabatic boundary condition is not taken into account. The environmental temperature of the test rig is 25°C.

The first dc test required energizing the winding from the experimental bench with a dc current of range 40-100 A. In the next test, the winding was powered with ac sinusoidal current of RMS 40-100 A at 50 Hz. In both tests, input voltage, current, power and temperature in the winding are monitored continuously.

During power loss measurements, proximity effects in a conductor are a consequence of the influence of an external time-varying magnetic field over the conductor and so a change in

the flow of the high frequency currents. In case there is an alternating current (ac), the proximity and skin effects will coincide, changing the current distribution and increasing the resistance of the conductor. The increasing winding resistance causes the winding temperature to increase. To monitor winding temperature four thermocouples are used and placed in the middle of active length and in the end-winding from both sides of the coil as shown in Figure 3a.

4. Finite element models

The effects of these disposed conductors are quantified numerically using 2-D and 3-D finite element analysis (FEA) software [8]. For this analysis, series arrangements of conductors with round wires in the slots were built as examples to illustrate distribution of losses within conductors. Accurate modelling of the whole winding including end-winding for ac loss calculation using finite element method (FEM) requires three-dimensional FEA. Analysis of the loss distribution within the stator core with coil is carried out using the established discrete time-step FEM, with both 2-D and 3-D formulations. Figure 4 illustrates a mathematical model of the stator core with wound winding assumed in the FEM calculations.

The discretisation mesh within the cross-section is the same for both 2-D and 3-D models and, for both used methods, calculations were assuming a constant winding reference temperature, set arbitrarily to 25°C. Due to symmetry, the study domain of FE stator models can be limited to half (symmetry in XY plane). The ferrite core size determines the large opening slot hence the copper losses in strands placed near the slot opening region are suspected to produce huge amount of eddy-current due to flux leakage [4, 10]. Winding losses can be reduced by properly arranged conductors and designed shape of teeth including the size of slot opening. Additionally, copper losses are dependent on electrical parameters such as operating frequency and drive wave-shape.

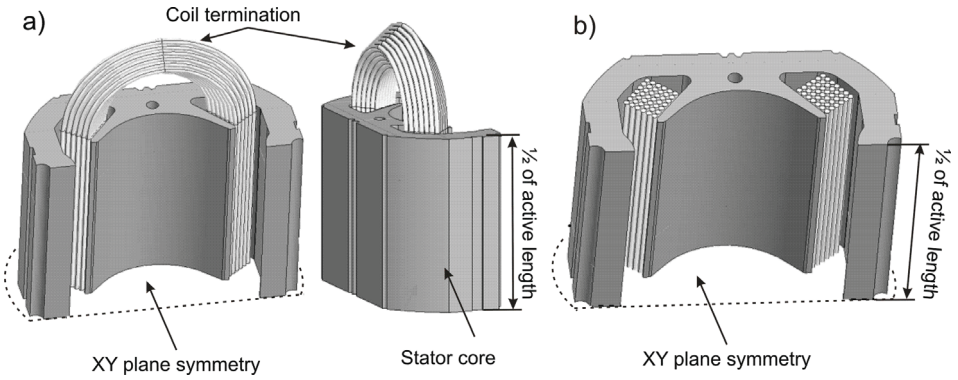

Fig. 4. 2-D (a) and 3-D (b) FE model for loss calculation – winding version I

The initial baseline arrangement of conductor in slot is listed as version I (see also Figs. 1 and 4). Outline of the cross-section stator core with different winding versions is shown in

Figure 5 and numbered sequentially version II through VII. Each winding version presents a coil, which includes 7 turns and is wounded using round wire with 6 strands in a bundle (∅1.6 mm). Distance between conductors for all winding arrangement cases is fixed (0.25 mm). Winding versions II, III, IV, and V were moved to the back of slot. The other winding versions were moved forward to the tooth-tip (version VI and VII). Six parallel conductor strands of winding versions I, II and III were formed in a rectangular profile as can be seen in Figure 5. The winding versions IV-VII consist of some strands randomly formed in the slot window.

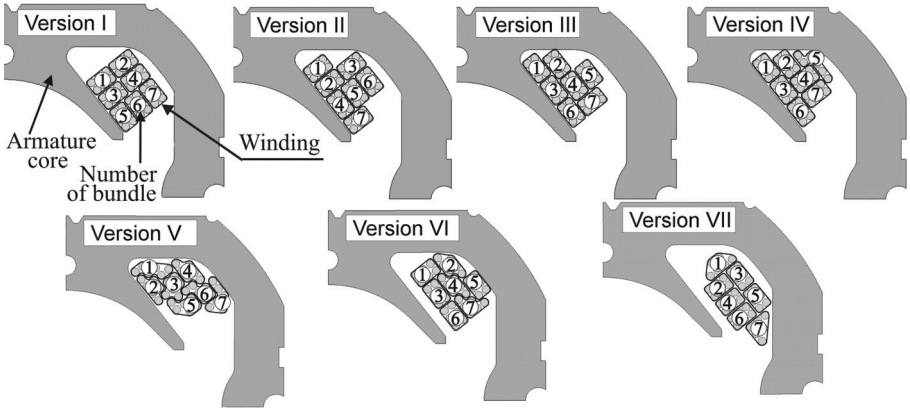

Fig. 5. Outline of the cross-section armature motor with seven versions of winding arrangements in the slot

Many references have reported the investigation of methods for copper loss reduction with round strands. Less attention has been paid to alternating loss reduction in winding with rectangular shape of conductors [14-16]. The value of the filling factor k_c in the analysed stator segment with the round conductors as in Figure 5 is 40%. Since the k_c depends on the winding wire and the slot geometry, it is difficult to state general values of the filling factor. Wound coil with round conductors (loose bundle) leads to lower filling factors than performed coils with rectangular shape. The filling factor k_c is an important design criterion regarding the motor efficiency. Higher k_c requires lesser current density for the same magnetomotive force and the smaller the dc copper losses are. Rectangular conductors are predominantly wound with their higher facing the stator pole. Moreover, rectangular conductors have a tendency to decrease ac loss [16]. To demonstrate the phenomena of loss reduction, two different arrangements of winding are investigated in respect to the ac resistance and copper losses at high frequency operation. Figure 6 shows an outline of the winding configurations with rectangular conductors 1.5 mm×4 mm, where coil includes 7 turns and is wound with 2 parallel strands in a bundle.

Upper and lower layers of the winding version VIII (Fig. 6a) and version IX (Fig. 6b) are wound with higher length of strand perpendicularly and radially to the tooth, respectively. The bending of the end turns is not critical for rectangular strands wound perpendicularly to the tooth. Rectangular conductors placed radially to the tooth require a more complicated tech-

nique for bending end-winding. This technique for winding the coil leads to minimization of eddy-currents (as will be shown in next section, Fig. 14). For the minimization of eddy-current loss, rectangular conductors should be wound with their higher edge facing the stator back-iron, even if the end-winding bending is technically more complex.

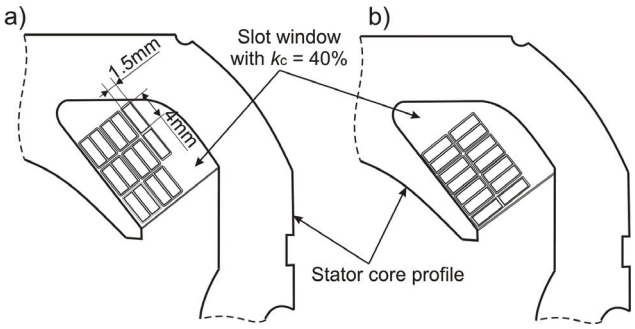

Fig. 6. Outline of the rectangular winding. Winding configuration with strands located perpendicularly with higher edge facing to tooth – version VIII (a) and located radially with higher edge facing to tooth – version IX (b)

The filling factor k_c of the rectangular strands was kept the same as for winding versions with round strands (versions I-VII), and the cross-section of each turn was the same in all winding versions presented in this paper.

5. Results

The total power losses as a sum of iron and copper losses for each winding version have been determined computationally and the results are plotted in Figure 7.

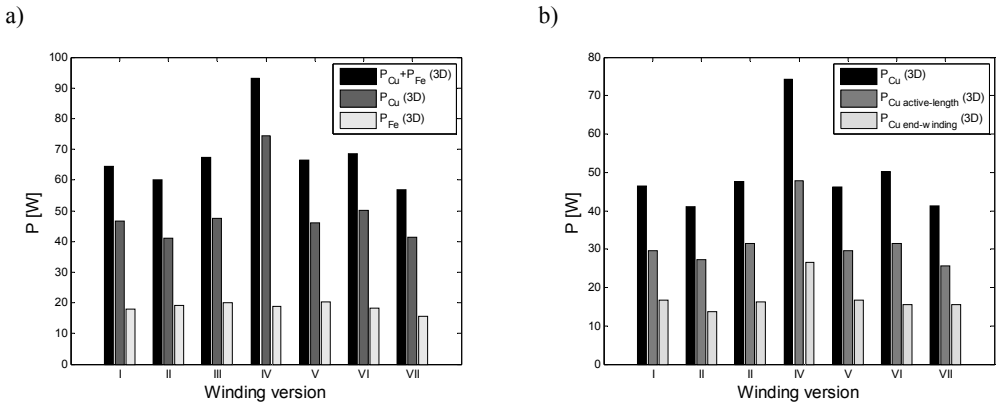

Fig. 7. 3-D FEA of iron and copper (a) and copper loss computed in slot and in coil termination (b) for different arrangements of winding at 800 Hz and I_{rms} = 80 A

The predicted separately losses in copper and iron for each investigated winding version are shown in Figure 7a. A lower total losses under ac RMS current 80 A at 800 Hz of the investigated winding arrangements is 57.6 W and 60.2 W obtained from the winding versions II and VII, respectively. A higher power loss at the same current and frequency operation is 93.14 W generated by the winding version IV. Thus, a reduction of losses by approx. 33-35.54 W was obtained by placing strands in the centre of the slot, and moved them further from the tooth side to back iron where flux leakage crossing the slot window is smaller [4]. Furthermore, end-winding may produce significant proximity losses and thus influence eddy-currents circulation in conductors [17]. Figure 7b shows copper losses in the slot ($P_{\text{Cu\_active-length}}$) and in the end-winding region ($P_{\text{Cu\_end-winding}}$) separately. It is easily noticed the end-winding generates lower loss than losses in the slot. Nevertheless, the amount of end-winding loss is significant and can not be omitted from ac loss prediction.

To demonstrate the "save window slot" area for strands with smaller impact of proximity effect the flux leakage lines pattern and values of flux density marked with dots in slot are depicted in Fig.8. In this particular case of ferromagnetic core profile, the worse scenario is to place strands near the slot opening by the tooth where more flux leakage is observed crossing the slot and thus the magnetic flux density is higher. Hence this pattern causes extra losses in strands.

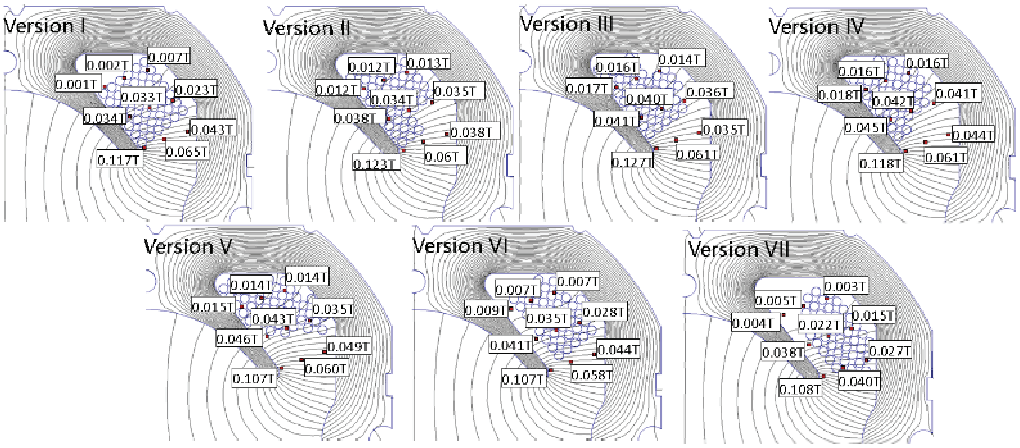

Fig. 8. Distribution of slot leakage and flux density values marked with dots in the slot at frequency 800 Hz under ac powered winding (RMS 80 A)

Figure 9 presents the alternating eddy-current distribution with the ratio of ac to dc copper losses in the winding for winding version II which produce the lower amount of ac losses and for winding version IV generating stronger proximity losses. In both cases the proximity loss is stronger in the open slot side due to higher leakage flux. Also this 2-D FE results show strands that can produce higher copper losses when them are laid with higher faces perpendicularly to flux leakage. For example, the considered winding versions in Figure 9 the ratio of resistive losses in strand in the left side of the open slot was changed from 10.11 (version II) to 13.82 (version IV) and consequently increased by 26.84% at 800 Hz, RMS 80 A.

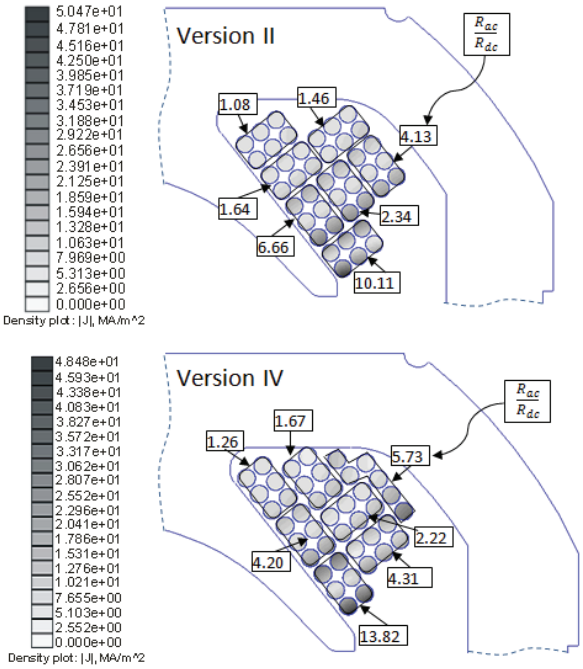

Fig. 9. Current density distribution with resistance ratio in each turn at RMS 80 A, 800 Hz for winding version II and IV

Figure 10 shows power loss dependence on frequency and current, calculated in both 2-D and 3-D FE method in iron and copper for winding version I. The copper losses predicted by 2-D FEA are lower than those for 3-D FEA as expected due to the fact that the 2-D models have not taken the end-winding effect into account. The iron losses (P_{Fe}) are insignificant for all the winding versions operating in the frequency range of 0-100 Hz at the ac current source. Over the frequency of 100 Hz, iron losses are rising with copper losses. The average difference between 2-D and 3-D prediction of total losses ($P_{Cu} + P_{Fe}$) for winding version I was some 24%.

To demonstrate the impact of the proximity effect from the end-winding region on the strands placed into the slot the 2-D prediction was provided and shown in Figure 11. This shows the effect of the physical phenomena associated with the resistance generated on the coil (winding version I). The ac resistance of the coil is composed of three components such as dc resistance, the resistance generated by the skin effect, and the resistance generated by the proximity effect. When an ac magnetic field is generated by ac high-frequency current, an electric field is generated. Then an effective resistance is produced when the current density becomes nonuniform. This effect (skin effect) was omitted due to used low diameter of strands. At high frequency the ac magnetic field generated in strands by the adjacent wire, an eddy- current flows (proximity effect). The resistance is rising due to the smaller cross-section. This amount of resistance rising can be demonstrated by the resistance ratio R_{ac} to R_{dc} as shown in Figures 9 and 11. The percent ratio of copper loss in the end-winding ($P_{Cu\_end\text{-}winding}$) to the total copper losses ($P_{Cu} = P_{Cu\_active\text{-}length} + P_{Cu\_end\text{-}winding}$) is 23% to 28% depending on a winding version.

a) b)

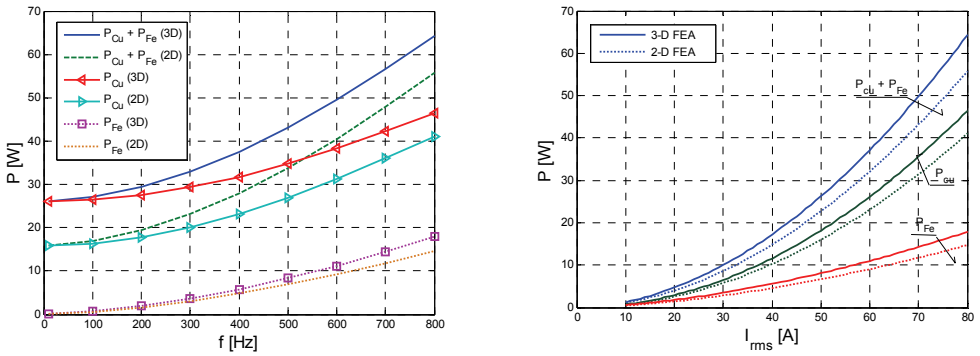

Fig. 10. 2-D and 3-D FE calculation of power loss for winding version I at 80 A_{rms} vs. frequency (a) and RMS current at 800 Hz (b)

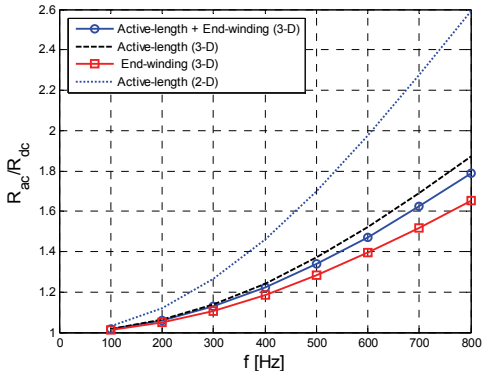

Fig. 11. The ratio of the equivalent ac resistance to the ideal dc value R_{ac}/R_{dc} vs. frequency at RMS 80 A

The ratio of ac to dc copper losses from the 3-D FE model for each winding version is shown in Table 2 for RMS 80 A current and high frequency operation. The increased resistance in the strands is particularly visible at high excitation frequencies. The minimum resistance rise was obtained for winding versions I and II (R_{ac}/R_{dc} = 1.52 and 1.62, respectively).

Table 2. 3-D FEA of resistance ratio at 800 Hz for RMS 80 A

Winding version	$\boldsymbol{R_{ac}/R_{dc}}$		
	P_{Cu}	$P_{Cu\ active\text{-}length}$	$P_{Cu\ end\text{-}winding}$
I	1.79	1.87	1.65
II	1.62	1.72	1.46
III	1.90	1.98	1.77
IV	2.99	3.01	2.97
V	1.81	1.86	1.73
VI	1.91	1.98	1.80
VII	1.52	1.62	1.38

The ac loss component contributes to a significantly higher operating temperature compared with the dc operation. Figure 12a shows results of total loss measurements obtained from coil presented in Figure 3 (winding version IV) under dc operation at an operating current range of 0-108 A and under ac operation at the frequency of 50 Hz at an operating current range of 0-108 A_{rms}. In this particular test of the investigated coil, the iron loss is insignificant and results clearly demonstrate that the copper losses are dominant.

a) b)

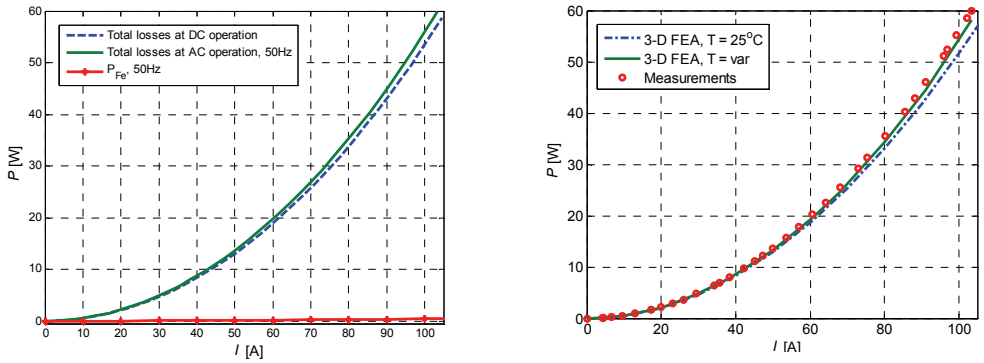

Fig. 12. 3-D FEA of power losses vs. dc and ac currents at 50 Hz (a), and measurements with 3-D FEA of power losses vs. ac current at 50 Hz (b) for winding version IV

The measurements of ac total power loss at 50 Hz were compared with 3-D FE calculation for winding version IV and it is shown in Figure 12b. To illustrate power loss dependence on temperature, two cases of 3-D FEA were considered. In the first stage the operating winding temperature was neglected and assumed to $T = 25°C$. In the second stage, the working temperature was taken into account to FEA. The results clearly confirm that the winding copper loss prediction can correlate with measurement in a good agreement only if the working temperature is taken into account. Finally, the calculated results show a good agreement with the experimental data.

Figure 13 shows an example of average temperature variation vs. time in the coil powered by ac current. It is crucial to measure temperature during tests of power losses or develops a thermal method to predict winding temperature e.g. a method based on the finite integration technique for the discretization, which gives an equivalent thermal model allowing the evaluation of transient temperature evolutions in the slot [11, 12]. The temperature was monitored at ac current and an operation frequency of 50 Hz. The temperature can rise faster and higher during the time when the winding operates in very high range of frequency [13]. Also, increasing current in the coil leads to enhanced temperatures in the strands. The curve in Figure 12b indicates that the distribution of power loss (eddy-currents) was not uniform in the copper (strands). Temperature is demonstrated to have a major impact on the proximity effect, as its magnitude is dependent on resistivity, which increases at elevated temperatures.

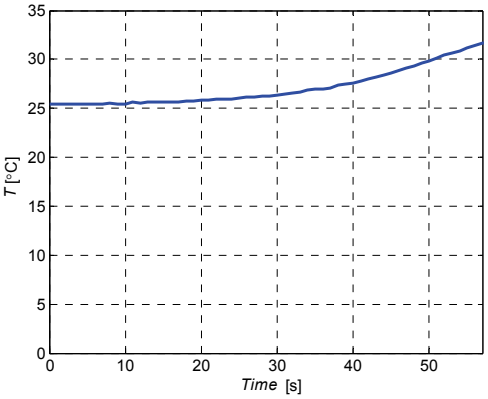

Fig. 13. Example of winding temperature changing vs. time under ac RMS current range of 0-108 A for frequency operation at 50 Hz

To demonstrate the influence of winding geometry on machine performance, two different winding arrangements with rectangular conductors were computed. Figure 14 shows 2-D FEA of the ratio of ac to dc copper losses. Eddy-currents inside of coil conductors increase strongly with the height of the conductors placed perpendicularly to the tooth as the winding version VIII shows. The resistance ratio in strands located close to the slot opening are significant and may be rapidly reduced by location of conductors with their higher edge facing the stator yoke as shows the winding version IX. A lower ac to dc resistance ratio indicates a slow change in motor winding temperature, which will affect the machine performance.

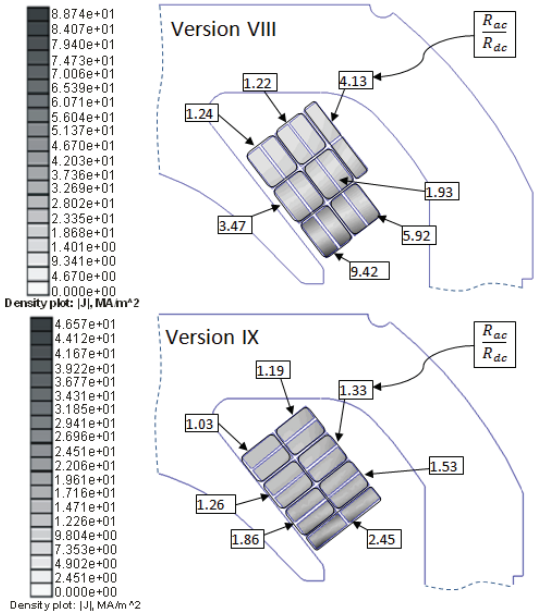

Fig. 14. Current density distribution with resistance ratio in rectangular conductors at RMS 80 A, 800 Hz for winding versions VIII and IX

Following the phenomena of changing the resistance ratio for these two winding versions VIII and IX, it becomes obvious that winding versions VII, II, I, V (having loose bundle

formed in rectangular shape with round conductors) have a tendency to minimize eddy-currents due to higher number of turns formed with their lower edge facing the tooth than the versions III, VI and IV (also with round conductors).

6. Conclusion

In this paper, a series of FE analyses have been carried out to investigate the influence of strands position in the slot on ac copper losses and iron losses. The operating frequency of the electric machine is the main parameter influencing the eddy-current. A higher operating frequency produces stronger skin and proximity effects in conductors.

An investigation of methods for calculating the ac proximity effects has been presented. The analysis accounts for both the active-length and end-winding regions. Loss prediction using 2-D and 3-D FEAs have been compared, showing that the simpler 2-D approach is insufficient to predict reasonable amount of the R_{ac}/R_{dc} ratio and/or winding losses (Figs. 10, 11). The results have shown that end-winding proximity losses are lower than those generated within the active-length of conductors, but are still significant. To account for the end-winding effect when using results from 2-D FEA, a 3-D FEA should be taken into account for the true path length of ac circulating currents within the conductor. To validate the theoretical findings, a thermal test was performed on a prototype stator tooth segment with wound coil to examine ac effects. Temperature and total power loss within the winding were recorded. The theoretical 3-D FE predictions have shown good agreement with the experimental data.

From the computation results shown in Figures 10a and 11, we can conclude that the ac copper losses increase with the frequency as expected. The ac resistance losses at 800 Hz are increased by 152-299% comparing to dc resistance losses according to the investigated winding version. Also, the minimum losses at high frequency range of 100-800 Hz are observed for winding versions II and VII, as compared to others. The results suggest that placed strands into the rear of slot and further from the slot corners where the flux leakage is dominant help to reduce ac copper losses. A size of the slot opening and its profile strongly determines a copper loss. The results also clearly demonstrate that the high-frequency ac copper loss varies with temperature in different manners to the dc winding resistance (Fig. 12b).

References

[1] Hendershot J.R., Miller T.J.E., *Design of brushless permanent-magnet machines*. Published in the USA by Motor Design Books LLC, 102 Triano Circle, Venice, Florida, 34292, USA (2010).
[2] Kazimierczuk M.K.: *High-frequency magnetic components*. (Wiley, 2nd edn. 2009)
[3] Wojda R.P., Kazimierczuk M.K., *Analytical optimization of solid-round-wire winding*. IEEE Transactions on Industrial Electronics 60(3): 1033-1041 (2013).
[4] Hiroki Shinagawa, Takayuki Suzuki, Masahiro Noda, Yusuke Shimura, Shigemi Enoki, Tsutomu Mizuno, *Theoretical analysis of AC resistance in coil using magnetoplated wire*. IEEE Transactions on Magnetics 45(9): 3251-3259 (2009).
[5] Iwasaki S., Deodhar R.P, Yong Liu et al., *Influence of PWM on the proximity loss in permanent-magnet brushless AC machines*. IEEE Transactions on Industry Applications 45(4): 1359-1367 (2009).

[6] Thomas A.S., Zhu Z.Q., Jewell G.W., *Proximity loss study in high speed flux – switching permanent magnet machine*. IEEE Transactions on Magnetics 45(10): 4748-4751 (2009).
[7] Carretero C., Acero J., Alonso R., Burdio J.M., Monterde F., *Embedded ring-type inductors modelling with application to induction heating systems*. IEEE Transactions on Magnetics 45(12): 5333-5343 (2009).
[8] Xi Nan, Sullivan C.R., *An equivalent complex permeability model for Litz-wire windings*. IEEE Transactions on Industry Applications 45(2): 854-860 (2009).
[9] Petkov R., *Optimum design of a high-power, high-frequency transformer*. IEEE Transactions on Power Electronics 11(1): 33-42 (1996).
[10] Cedrat: *Flux3D*. User's Guide 3 (2008).
[11] Wu L.J., Zhu Z.Q., Staton D. et al., *Analytical model of eddy current loss in winding of permanent-magnet machines accounting for load*. IEEE Transactions on Magnetics 48(7): 2138-2151 (2012).
[12] Jinxin Fan, Chengning Zhang, Zhifu Wang et al., *Thermal analysis of permanent magnet motor for the electric vehicle application considering driving duty cycle*. IEEE Transactions on Magnetics 46(6): 2493-2496 (2010).
[13] Idoughi L., Mininger X., Bouillault F., Bernard L, Hoang E., *Thermal model with winding homogenization and FIT discretization for stator slot*. IEEE Transactions on Magnetics 47(12): 4822-4826 (2011).
[14] Farahmand F., Dawson F.P, Lavers J.D., *Temperature rise and free-convection heat-transfer coefficient for two-dimensional pot-core inductors and transformers*. IEEE Transactions on Industry Applications 45(6): 2080-2089 (2009).
[15] Wallmeier P., *Improved analytical modelling of conductive losses in gapped high-frequency inductors*. IEEE Transactions on Industry Applications 37(4): 1045-1054 (2011).
[16] Waseem A, Roshen, *High-frequency fringing fields loss in thick rectangular and round wire winding*. IEEE Transactions on Magnetics 44(10): 2396-2401 (2008).
[17] Mellor P.H., Wrobel R., McNeill N., *Investigation of proximity losses in a high speed permanent magnet motor*. IEEE Industry Applications Conference, pp. 1514-1518 (2006).
[18] Wrobel R., Mlot A., Mellor P.H., *Contribution of end-winding proximity losses to temperature variation in electromagnetic devices*. IEEE Transactions on Industrial Electronics 59(2): 996-1003 (2010).